

Ultrasonic Wave Propagation in Doped *n*-Germanium and *p*-Silicon

WARREN P. MASON AND T. B. BATEMAN

Bell Telephone Laboratories, Murray Hill, New Jersey

(Received 9 January 1964)

The effect of doping germanium with *n*-type material and silicon with *p*-type material is to increase the attenuation and decrease the elastic moduli. The decrease in the c_{44} elastic modulus for *n*-type germanium agrees fairly well with theoretical predictions. However, the modulus decrease in *p*-type silicon is much larger and varies with temperature much faster than predicted by any present theory. It is suggested that there is a temperature-induced change in hole population along the energy surfaces. The intervalley relaxation time, which determines the added attenuation, becomes independent of the doping for high dopings with the antimony time being about 100 times that for arsenic. This result indicates that the relative values are determined by the square of the triplet singlet separation which occurs near the impurity atoms. For *p*-type silicon the relaxation time at low temperatures increases very markedly indicating an activation-energy effect. The energies agree well with the energies measured by infrared techniques for the largest excited state orbits around the impurity atoms. The relaxation times measured at high temperatures indicate that the hole is transported $\frac{1}{3}$ cycle from one $\langle 111 \rangle$ position to the next.

I. INTRODUCTION

It was first pointed out by Keyes¹ that the introduction of arsenic, phosphorus, or antimony into germanium—*n*-type doping—produces a decrease in the shear elastic modulus c_{44} . The result was shown to be due to the effect of the electronic part on the strain energy function and to involve only those electrons which change from one valley to another. The experimental results of Keyes and Bruner showed that the measured decrease was about 75% of the calculated decrease and varied with temperature as predicted by theory.

Pomerantz, Keyes, and Seiden² showed that the finite time required for electrons to go from one valley to another was a relaxation effect and should result in an attenuation of sound waves at a high frequency. Measurements at 9 kMc/sec did show² an absorption so high that it could not be quantitatively determined for any wave involving the c_{44} elastic modulus, while normal phonon-phonon attenuation resulted for any mode not involving this elastic constant.

II. EFFECT OF DOPING GERMANIUM WITH *n*-TYPE MATERIAL

A. Experimental Results

By going to 500 Mc/sec, or less, measurable results were obtained³ for arsenic doping. The present paper extends these results to antimony and phosphorus doping. These data are of considerable interest in delineating the mechanisms causing changes of electrons from one valley to another and the relaxation times for these processes. Hence, they have been rather extensively investigated.

Figure 1 shows the increased attenuation for longitudinal waves along the $\langle 110 \rangle$ direction caused by

¹ R. Keyes, I.B.M. J. Res. Develop. **5**, 266 (1961); L. J. Bruner and R. W. Keyes, Phys. Rev. Letters **7**, 55 (1961).

² M. Pomerantz, R. W. Keyes, and P. E. Seiden, Phys. Rev. Letters **9**, 312 (1962).

³ W. P. Mason and T. B. Bateman, Phys. Rev. Letters **10**, 151 (1963).

doping germanium with 10^{18} and 3×10^{19} arsenic atoms per cc. The measurements were made at a frequency of 475 Mc/sec. The difference between the attenuation of the doped and pure crystal is practically independent of the temperature. The elastic modulus is determined by the sum

$$c = (c_{11} + c_{12} + 2c_{44})/2. \quad (1)$$

Since it has been shown^{1,3} that the only elastic constant that is affected by *n*-type doping of germanium is c_{44} , the attenuation can be ascribed to the results of a resolved shearing stress associated with the longitudinal wave. In fact the attenuation is caused by the finite relaxation time associated with the motion of electrons between the four valleys of the energy surface of *n*-type germanium. It satisfies the relaxation equation

$$A_{(N_D/cm)} = (\Delta c_{44}/2\rho V^3)(\omega^2\tau), \quad (2)$$

valid when $\omega\tau \ll 1$ and $(\omega/V)\lambda < 1$, where λ is the mean free electron path. In this equation Δc_{44} is the change in modulus caused by the doping, ω is $2\pi f$, ρ the density, and V the velocity for the longitudinal wave. Changes in the c_{44} modulus for a doping of 3×10^{19} boron atoms per cc were measured by Bruner and Keyes¹ with the results shown by Fig. 2. This change was determined by the difference in velocities for pure and doped samples measured at 10 Mc/sec. The dashed curve shows the calculated value—from Eq. (13)—for the sample doped with 10^{18} arsenic atoms per cc. Measurements for antimony-doped germanium, shown by Fig. 4, give a very similar change.

The attenuation measurements of Fig. 1 and the velocity measurements of Fig. 2 can be used to determine the relaxation times, which are

$$\tau = 4 \times 10^{-13} \text{ sec}; \quad \tau = 2.3 \times 10^{-13} \text{ sec}, \quad (3)$$

respectively, for dopings of 10^{18} and 3×10^{19} arsenic atoms per cc. These times are shown plotted on Fig. 3. On account of the small change in attenuation, this method cannot be used to investigate dopings less than 10^{18}

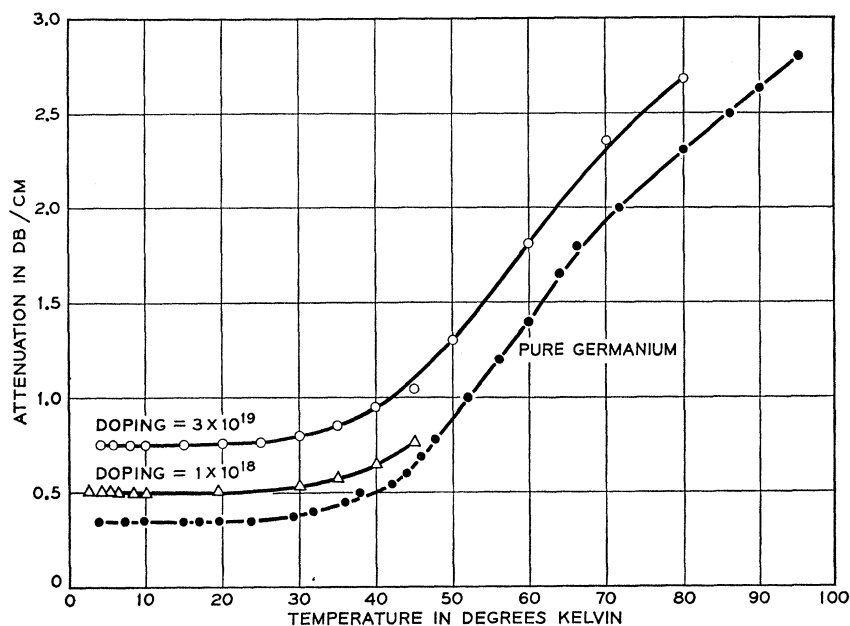


FIG. 1. Attenuation measurements of pure and arsenic-doped germanium. Longitudinal waves along $\langle 110 \rangle$, frequency 475 Mc/sec.

arsenic atoms per cc. However, another method applicable for lower dopings is the acousto-electric voltage method of Weinreich *et al.*⁴ Figure 3 shows the relaxation times for a number of doping levels from 10^{14} to 10^{16} arsenic atoms per cc. At low temperatures the relaxation time is determined by impurity scattering and the solid line of Fig. 3 shows the values obtained as a function of doping using the 40°K values.⁴ As the temperature increases, scattering occurs also by collisions with phonons and the dashed lines of Fig. 3 show the modification caused by this type of scattering for the temperatures shown.

The relaxation time for germanium doped lightly with arsenic impurities has been discussed by Weinreich

*et al.*⁴ as being due to a combination of scattering by neutral and ionized atoms. At low temperatures neutral scattering predominates and this gives a time inversely proportional to the impurity density. If we extrapolate this down to an impurity density of 10^{18} , the indicated relaxation time of 2×10^{-13} is less than the measured value of about 4×10^{-13} sec. For a density of 3×10^{19} the relaxation time approaches the value of 2.3×10^{-13} sec, which appears to be an intrinsic time for going from one valley to another.

An even stronger indication of this effect is furnished by antimony-doped germanium. Figure 4 shows the modulus and attenuation difference between a pure germanium sample and a sample doped with 1.5×10^{18}

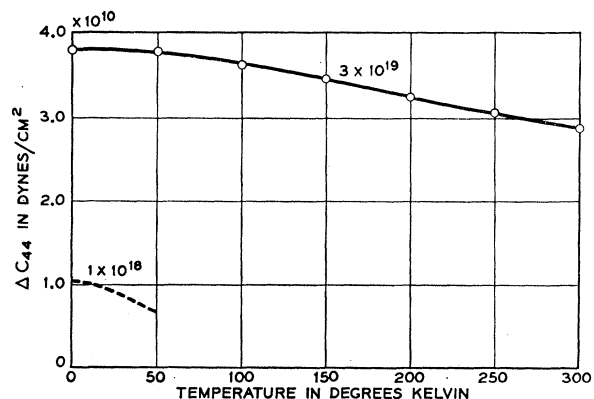


FIG. 2. Change in the elastic modulus c_{44} for arsenic-doped germanium. Measurements made at 10 Mc/sec. Dashed curve shows estimated value for a doping of 1×10^{18} arsenic atoms per cc (after Bruner and Keyes).

⁴ G. Weinreich, T. M. Sanders, and H. G. White, *Phys. Rev.* **114**, 33 (1959).

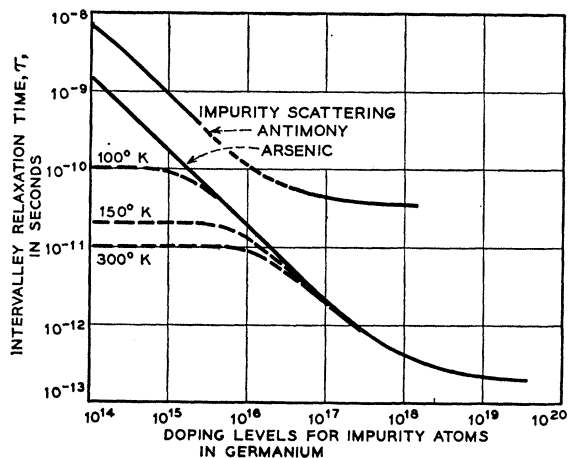


FIG. 3. Relaxation times for arsenic- and antimony-doped germanium as a function of doping. Dashed curves show effect of phonon scattering while solid curves are for impurity scattering.

antimony atoms per cc. The attenuation is so high for this sample that a measuring frequency of 99 Mc/sec was used. As before the measurements were made along a $\langle 110 \rangle$ direction for longitudinal waves. The relaxation time calculated from these measurements is shown plotted by the dashed line of Fig. 4. At low temperatures impurity scattering is dominant and a value of 3.8×10^{-11} sec results. As the temperature is increased, phonon scattering occurs and the value approaches the same value found for arsenic doping at 300°K. The values for impurity doping by antimony are shown by Fig. 3. Another measurement was made for a doping of 10^{17} giving the value of the relaxation time, as shown. Measurements for lower doping have been made by Tell and Weinreich.⁵ The results quoted indicate a relaxation time five times as large as that for antimony doping over a range from 10^{14} to 2.5×10^{15} atoms per cc. The resulting relaxation time for the entire range is shown by Fig. 3.

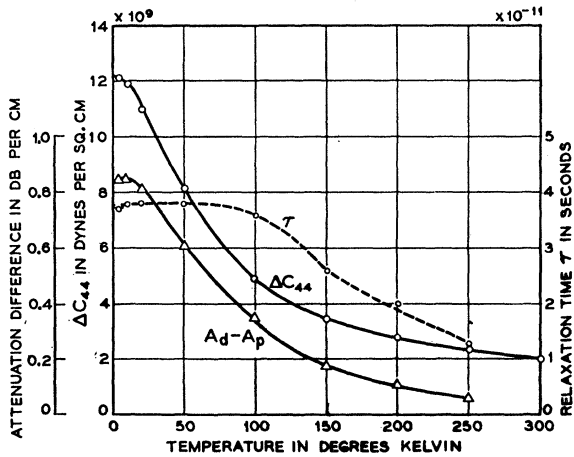


FIG. 4. Attenuation and modulus changes for germanium doped with 1.5×10^{18} antimony atoms per cc. Measurements made at 99 Mc/sec. Dashed line shows corresponding relaxation time.

Here the constancy of the intervalley relaxation time is confirmed over a wide doping range.

B. Theoretical Interpretation

Many experimental results for *n*-type germanium and silicon have been interpreted in terms of the many-valley model of the energy surfaces. Figure 5 shows the energy surfaces for silicon and it is seen that for the conduction band, one of the surfaces has a very low energy value in *k* space along the $\langle 100 \rangle$ axis. Electrons tend to congregate about these momentum values. Since there are six $\langle 100 \rangle$ directions, there are six energy minima or valleys. The six surfaces are shown by Fig. 6. The ovals indicate surfaces of constant energy. Similar considerations apply to the conduction band for germanium except that the minimum energy directions lie

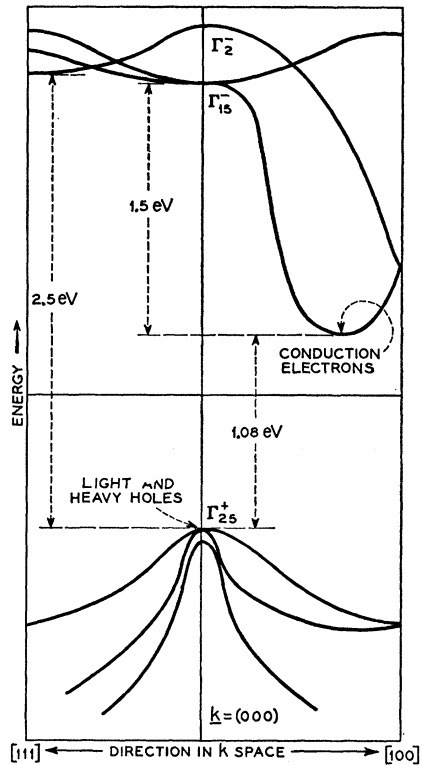


FIG. 5. Energy surfaces in valence and conduction band for silicon.

along $\langle 111 \rangle$ axis and occur at the edges of the Brillouin zone.

In the unstressed condition all the valleys have equal energies and electron populations. The effect of a

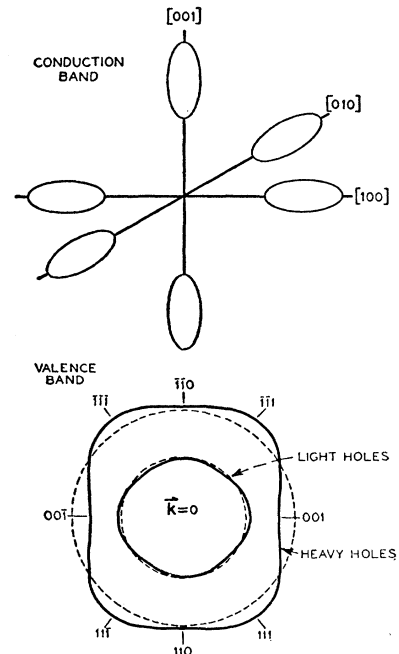


FIG. 6. Top figure: multivalley energy surfaces for *n*-silicon. Bottom figure: cross section of energy surfaces a constant distance below the origin.

⁵ B. Tell and G. Weinreich, Bull. Am. Phys. Soc. 7, 546 (1962).

stress T_1 along a crystal axis in silicon is to raise the energy of the parallel valleys and lower those of the perpendicular valleys by amounts $\frac{2}{3}\Phi S_1$ and $-\frac{1}{3}\Phi S_1$, respectively, where S_1 is the longitudinal strain induced by the applied stress and Φ is the deformation potential. This causes electrons in the parallel valleys to flow into the perpendicular valleys. In the nondegenerate range the equilibrium ratio of population is determined by Boltzmann's principle

$$N_{100}/N_{010} = \exp(-\Phi S_1/kT). \quad (4)$$

This, together with the conservation of electrons given by

$$N_0 = 2N_{(100)} + 4N_{010}, \quad (5)$$

determined the equilibrium populations to be

$$2N_{100} = \frac{N_0 \exp(-\Phi S_1/kT)}{2 + \exp(-\Phi S_1/kT)} \doteq \frac{N_0}{3} \left[1 - \frac{2\Phi S_1}{3kT} \right]; \quad (6)$$

$$4N_{010} = \frac{2N_0}{2 + \exp(-\Phi S_1/kT)} \doteq \frac{2N_0}{3} \left[1 + \frac{\Phi S_1}{3kT} \right].$$

The change in energy ΔW caused by the applied stress is given by

$$\Delta W = \frac{N_0}{3} \left[1 - \frac{2\Phi S_1}{3kT} \right]^2 \Phi S_1 - \frac{2N_0}{3} \left[1 + \frac{\Phi S_1}{3kT} \right] \frac{\Phi S_1}{3}$$

$$= -\frac{2N_0 \Phi^2 S_1^2}{9 kT}. \quad (7)$$

There is no change to first powers of the strain but a negative contribution occurs proportional to the square of the strain. If we add this to the elastic energy $\frac{1}{2}c_{11}S_1^2$, it is seen that a lowering of the elastic modulus occurs of a value

$$\Delta c_{11} = -\frac{4N_0\Phi^2}{9kT}; \quad (8)$$

also

$$\Delta c_{12} = -\frac{\Delta c_{11}}{2} = \frac{2N_0\Phi^2}{9kT}; \quad \Delta c_{44} = 0.$$

The last two relations follow since a shearing strain affects all the wells in the same fashion while a stress along $\langle 111 \rangle$ direction also affects all the valleys equally. Since the elastic constant for this direction is $(c_{11} + 2c_{12} + 4c_{44})/3$, the second relation of (8) must hold.

For n germanium, a similar calculation¹ shows that

$$\Delta c_{11} = \Delta c_{12} = 0; \quad \Delta c_{44} = -(N_0/9)(\Phi^2/kT) \quad (9)$$

in the nondegenerate range. For the degenerate range the limiting value of Δc_{44} is obtained by replacing kT by two-thirds of the Fermi energy or

$$\frac{2}{3}W_F = (\hbar^2/3m^*)(3\pi^2N)^{2/3}, \quad (10)$$

where \hbar is Plank's constant h divided by 2π , N is the number of free electrons, which is equal to the number of impurity atoms in the degenerate range, and m^* the density of states mass

$$m^* = (m_l m_t^2)^{1/3} (n)^{2/3}, \quad (11)$$

where m_l is the longitudinal mass of a single valley, m_t the transverse mass, and n the number of valleys. Inserting the value in (9), the limiting value of Δc_{44} at low temperatures is given by

$$\Delta c_{440} = -\frac{4}{3} \left(\frac{4\pi}{3} \right)^{2/3} \frac{N^{1/3} \Phi^2 (m_l m_t^2)^{1/3}}{\hbar^2}. \quad (12)$$

Since $m_l = 1.57m_0$; $m_t = 0.082m_0$, where m_0 is the electron mass 9.1×10^{-28} g, this equation takes the form

$$\Delta c_{440} = -1.58 \times 10^{25} \Phi^2 N^{1/3}. \quad (13)$$

From piezoresistance measurements and from other effects Φ is usually taken as 16 eV at room temperature. For very low temperatures 19 eV is more probable which corresponds to 3.04×10^{-11} ergs. Hence,

$$\Delta c_{440} = 1.44 \times 10^4 N^{1/3}. \quad (14)$$

This equation checks quite well with the measured values of Figs. 2 and 4 where the theoretical values are 4.7×10^{10} and 1.65×10^{10} dyn per square cm, respectively.

At the degeneracy temperature, given by

$$kT_D = W_F \quad \text{or} \quad T_D = \frac{\hbar^2 (3\pi^2 N)^{2/3}}{2m^* k}$$

$$= 7.61 \times 10^{-11} N^{2/3}, \quad (15)$$

the change in modulus should be one-half of Δc_{440} .¹ The curves of Fig. 4 indicate a value of $T_D = 80^\circ\text{K}$ compared to the calculated value of 99°K . Over a temperature range the ratio of Δc_{44} to Δc_{440} follows the relation¹ shown by Fig. 7. Using $T_D = 80^\circ\text{K}$ for Fig. 4, the agreement with the measured value is excellent.

The attenuation A is determined by the product of Δc_{44} and the relaxation time τ which is the time required to go from one valley to another. Measured values are

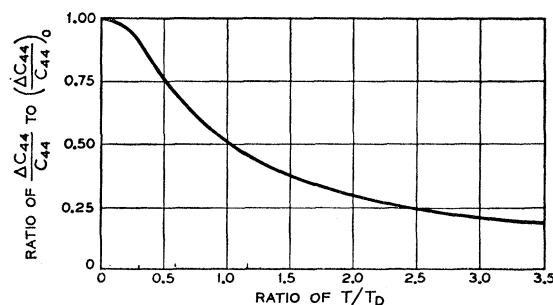


FIG. 7. Calculated ratio of $\Delta c_{44}/\Delta c_{440}$ as a function of the ratio of the temperature to the degeneracy temperature (after R. W. Keyes).

shown by Fig. 3. A number of different mechanisms determine this time. For dopings from 10^{14} to 10^{16} and temperatures above 150°K , the scattering mechanism is the collision of electrons with phonons. The total relaxation time, as determined by the conductivity equation, is given by

$$\tau = m^* \sigma / N e^2 = \mu m^* / e = 0.37 \times 1.1 \times 10^{-31} / 1.6 \times 10^{-19} \\ \doteq 2.5 \times 10^{-13} \text{ sec}, \quad (16)$$

where σ is the conductivity in mho/meter, N the number of electrons per cubic meter, e the electronic charge of 1.6×10^{-19} C, μ the mobility in $\text{M}^2/\text{V sec}$, and m^* the effective drift mass in kilograms. Using the values for lightly doped samples, the indicated value is about 2.5×10^{-13} sec at 300°K . Hence, about one in every 40 collisions results in a change in valleys.

As the temperature becomes lower, or the doping higher, the intervalley relaxation time is controlled by scattering from impurities. For low dopings this process has been discussed by Weinreich *et al.*⁴ as being due to a combination of scattering by neutral and ionized arsenic atoms. At low temperatures neutral scattering predominates and this gives a time inversely proportional to the impurity density. Scattering is probably due to elastic scattering by the impurity atoms which follows⁶ a law

$$1/\tau = \pi N R^2 V, \quad (17)$$

where N is the density of impurity atoms per cc, R the effective radius, and V the electron velocity. At 40°K the indicated cross section R^2 is about 5×10^{-13} cm^2 . This is attributed^{4,7} to an exchange interaction between valleys although no values are given.

As the temperature increases some of the arsenic atoms become ionized and a component is found which varies inversely as the electron density. This component, which has a strong temperature variation, is attributed^{4,7} to a capture of electrons in bound donor states followed by re-emission in another valley. As will be shown in the next section, this process has an activation energy and hence the time between capture and re-emission decreases as the temperature increases.

For densities above 10^{18} , the data of Figs. 1 and 4 show that there is no activation energy for the process and the data of Fig. 3 show that the relaxation time tends to reach a constant value independent of the doping level. All of the impurity atoms will be ionized since Fermi degeneracy⁸ occurs in germanium at an impurity concentration between 10^{17} and 10^{18} impurity atoms per cc. The impurities for degeneracy⁹ are in the order of 10^{17} for antimony and 5×10^{17} for arsenic

doping. Hence, bound donor states do not exist for these dopings.

In the neighborhood of an impurity atom the four degenerate energy minima are split into a singlet and triplet states by the valley-orbit splitting. The separations caused by antimony, phosphorus, and arsenic are 0.57×10^{-3} , 2.9×10^{-3} , and 4.15×10^{-3} eV, respectively. One mechanism proposed for the interchange of electrons between valleys is a "giant trapping"¹⁰ of electrons which involves a change in momentum between valleys by means of an interaction between the triplet and singlet states. If the electron is placed in the $1s$ state and simultaneously in a known valley, it will not be in a stationary state, but in a linear combination. At a later time, depending on the relative phases of the singlet and triplet state, the electron will be in a different valley. Weinreich *et al.*⁴ have estimated that the relaxation time for such a valley change should be

$$\tau \geq (16/3) (\hbar/\delta E) = 8.4 \times 10^{-13} \text{ sec (arsenic)} \\ = 6.14 \times 10^{-12} \text{ (Sb)}. \quad (18)$$

These values are too large for arsenic-doped germanium and too small for antimony-doped germanium.

Another derivation¹¹ indicates that the relaxation time should be in the ratio of the squares of the singlet-triplet separation and this is in better agreement with the experimental values. However, since this is essentially an elastic scattering process, the independence of the scattering time versus impurity density is still anomalous. The same is true for the total scattering time of Eq. (17). This time varies from 6 to 2×10^{-14} sec for the doping ranges from 10^{18} to 3×10^{19} impurity atoms per cc. The ratios of the intervalley to total scattering times are about 10 for arsenic and about 1000 for antimony.

III. EFFECT OF DOPING SILICON WITH *p*-TYPE MATERIALS

A. Experimental Results

Measurements have also been made of the effect of doping silicon with the *p*-type materials boron and gallium. The first measurements³ were made for 2.5×10^{18} boron atoms per cc. Measurements were made for longitudinal waves along the $\langle 110 \rangle$ and $\langle 100 \rangle$ directions and shear waves along $\langle 110 \rangle$ with polarizations along $\langle 001 \rangle$ —which involves the shear modulus c_{44} —and with polarization along $\langle 1\bar{1}0 \rangle$ which involves the $(c_{11} - c_{12})/2$ elastic modulus. As shown by Fig. 8(a), curve A, the attenuation for shear waves along $\langle 100 \rangle$ increases very markedly at low temperatures and becomes so high below 6°K and for a 475 Mc/sec frequency,

⁶ A. H. Wilson, *The Theory of Metals* (Cambridge University Press, New York, 1958), p. 10.

⁷ P. J. Price and R. L. Hartman (to be published) have recently given a derivation which accounts for the scattering of ionized arsenic atoms in germanium.

⁸ F. J. Morin and J. P. Maita, *Phys. Rev.* **96**, 28 (1954).

⁹ H. Fritzche, *Phys. Rev.* **125**, 1552 (1962).

¹⁰ M. Lax, *Phys. Rev.* **119**, 1502 (1960).

¹¹ P. J. Price, *J. Appl. Phys.* **31**, 849 (1960); measurements have recently been made for one value (1.5×10^{18}) of doping by phosphorus atoms in germanium. The value of 8×10^{-13} sec is intermediate between As and Sb and agrees well with the square of the singlet-triplet separation.

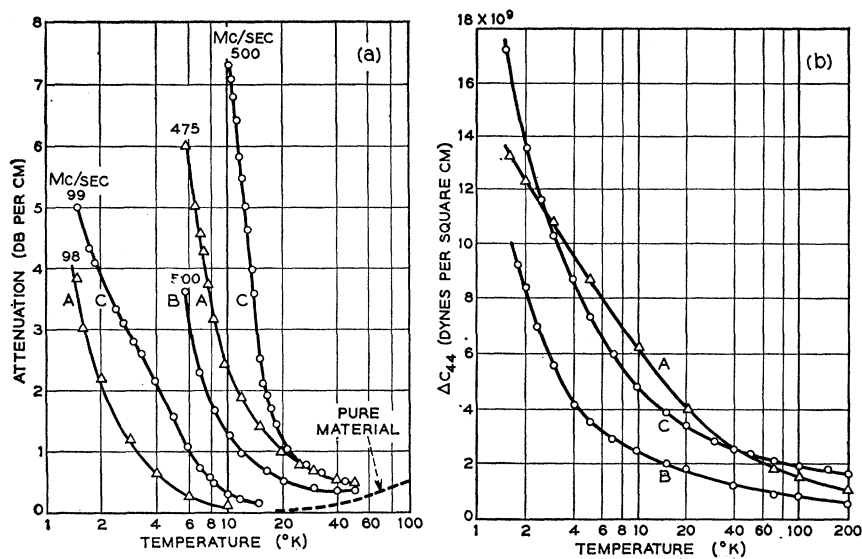


FIG. 8. (a) Measured attenuation as a function of temperature for A (2.5×10^{18} boron atoms per cc), B (5×10^{17} boron atoms per cc), C (1.5×10^{18} gallium atoms per cc). (b) Measured changes in the c_{44} elastic constants for the same conditions.

that it could not be measured. The frequency was shifted to 98 Mc/sec and the curve was measured from 1.5 to 15°K. In the overlap region, it is seen that the attenuation is square law as indicated by the relaxation Eq. (2).

Velocity measurements for pure and doped silicon were made by the pulse overlap method,¹² which is

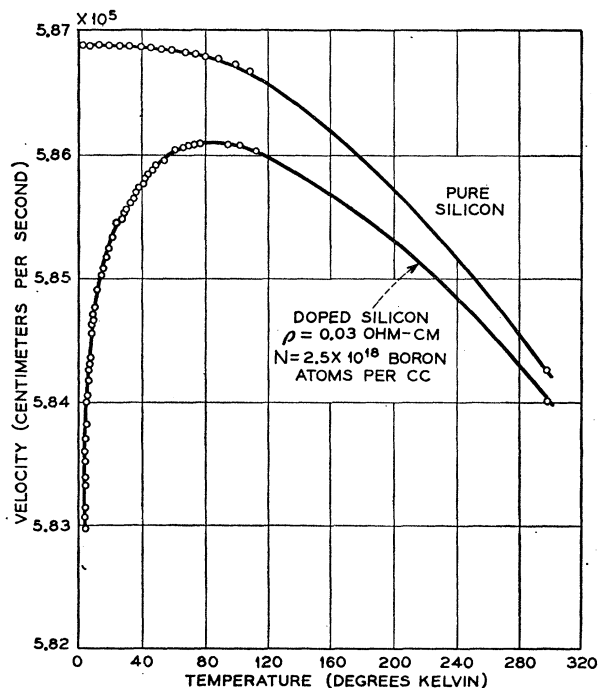


FIG. 9. Measured shear wave velocities along $\langle 100 \rangle$ direction for pure silicon and silicon doped with 2.5×10^{18} boron atoms per cc. Measurements made at 20 Mc/sec.

¹² H. J. McSkimin and P. Andreatch, J. Appl. Phys. 34, 609 (1962).

capable of good precision. Figure 9 shows the measured velocities for pure and doped samples. From these measurements, the change in modulus Δc_{44} can be determined and it is shown plotted by Fig. 8(b), curve A. The relaxation time from the measured attenuation and modulus differences can be calculated by using Eq. (2). The result is shown plotted on Fig. 10, curve A. For temperatures above 8°K the relaxation time satisfies the equation

$$\tau_1 = 1.3 \times 10^{-12} e^{13/T}, \quad (19)$$

indicating an activation energy δE of 0.00113 eV. At lower temperatures the curve bends off and approaches

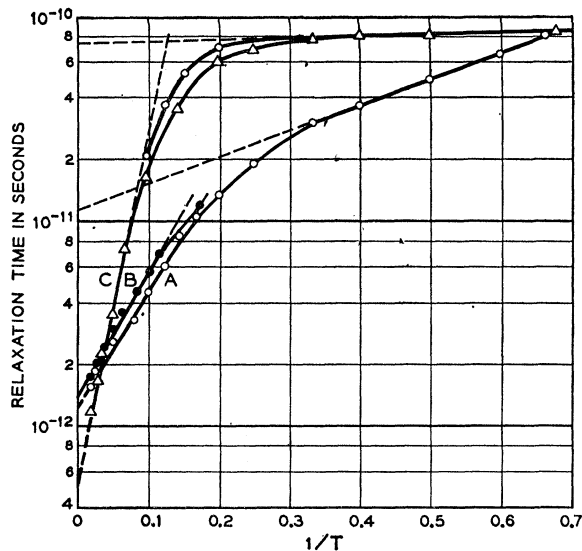


FIG. 10. Relaxation times for p -doped silicon plotted against $1/T$. A (2.5×10^{18} boron atoms per cc); B (5×10^{17} boron atoms per cc); C (1.5×10^{18} gallium atoms per cc).

another straight line having an equation

$$\tau_1' = 1.13 \times 10^{-11} e^{2.95/T}; \quad \delta E = 2.56 \times 10^{-4} \text{ eV}. \quad (20)$$

Detailed measurements were also made for longitudinal waves along the $\langle 100 \rangle$ direction with the results shown by Fig. 11. Here an increase in both attenuation and modulus change occurred as the temperature decreased, but their ratio, which determines the relaxation time, is approximately constant with a value $\tau_2 = 4.2 \times 10^{-12}$ sec.

The shear wave measurements along $\langle 110 \rangle$ with polarization along $\langle 1\bar{1}0 \rangle$ and the longitudinal measurements along $\langle 110 \rangle$ confirmed the expected relation that

$$\Delta c_{12} = -\Delta c_{11}/2. \quad (21)$$

The attenuations for these modes satisfy, respectively, the equations

$$A = \frac{\frac{3}{4} \Delta c_{11} \omega^2 \tau_2}{2\rho V_s^3}; \quad A = \frac{[(\Delta c_{11}/4)\tau_2 + \Delta c_{44}\tau_1]\omega^2}{2\rho V_l^3}. \quad (22)$$

The relaxation time τ_1 for shear waves along $\langle 100 \rangle$ has an activation energy term. In order to determine the origin of this term, measurements were made for a range of boron doping from 5×10^{17} to 3×10^{19} atoms per cc. Figures 8(a) and (b), curves B, show the results for shear waves along $\langle 100 \rangle$ measured at 500 Mc/sec for the doping of 5×10^{17} . The relaxation time is shown plotted on Fig. 10, with an indicated activation energy of 0.00117 eV or nearly the same as for the higher doping. The curves of Figs. 12 and 13 show the attenuation and velocities for the dopings of 10^{19} and 3×10^{19} boron atoms per cc. The lower value still has an increase in attenuation as the temperature is lowered, but the

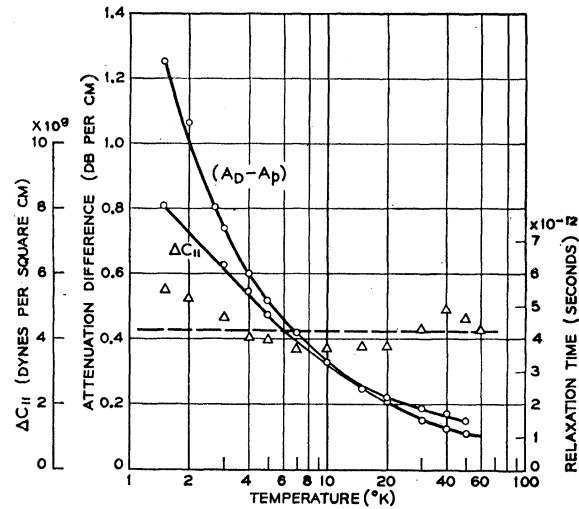


FIG. 11. Attenuation and modulus change Δc_{11} for longitudinal waves along the $\langle 100 \rangle$ axis. Dashed line shows an average relaxation time.

higher doping value has an added attenuation which is independent of the temperature with no activation energy. The doping of 10^{19} satisfies the relaxation equation

$$\tau_1 = 2.1 \times 10^{-13} e^{4/T}, \quad (23)$$

while the relaxation time for the doping of 3×10^{19} is 10^{-13} seconds independent of the temperature.

In order to complete the interpretation, a measurement was made for a doping of 1.5×10^{18} gallium atoms per cc in a $\langle 100 \rangle$ silicon crystal. Measurements were made for shear waves in this direction at a frequency of 500 Mc/sec. The results for the attenuation and

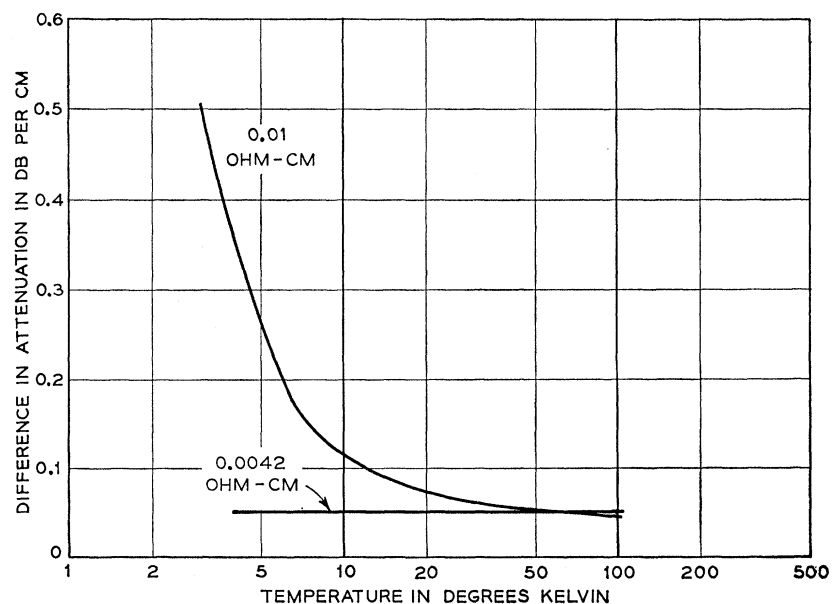


FIG. 12. Attenuation measured at 500 Mc/sec for boron-doped silicon as a function of the temperature. The curve labeled 0.01 Ω -cm is for a doping of 10^{19} boron atoms per cc while the one labeled 0.0042 is for 3×10^{19} boron atoms per cc.

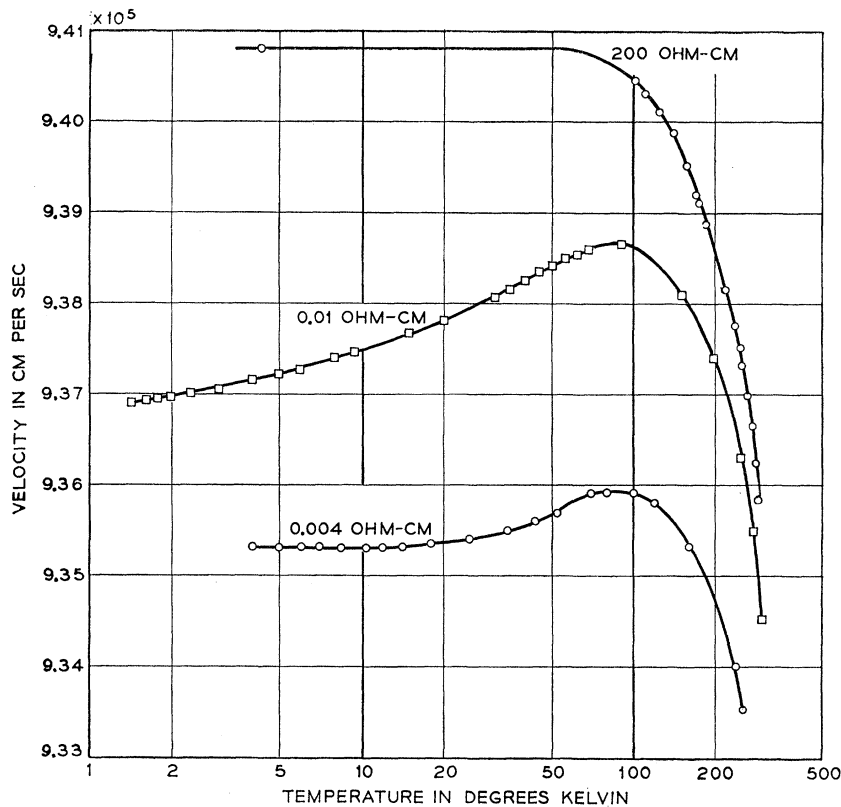


FIG. 13. Measured velocities for pure and doped silicon samples as described in Fig. 12.

modulus changes are shown by Figs. 8(a) and (b) by the curve labeled C. In the lower temperature range, measurements of the attenuation were made down to 1.5°K for a frequency of 99 Mc/sec. A plot of the relaxation time is shown by Fig. 10, curve C. The initial part of the relaxation time satisfies the equation

$$\tau_1 = 5 \times 10^{-13} e^{40/T} \text{ sec}, \quad (24)$$

giving an activation energy δE of 0.0035 eV. At lower temperatures the relation becomes curved but ends up with another straight line τ_1' which has a very low or zero activation energy. For intermediate temperatures the points agree fairly well with the equation

$$1/\tau = 1/\tau_1 + 1/\tau_1'. \quad (25)$$

B. Theoretical Interpretation

The interpretation for the relaxation time for the p region appears straightforward. Since the degeneracy temperature is 50°K or higher for all the doping levels used, the valence bands are filled up to 0.004 eV or higher above the band minima. Hence, it is believed that the relaxations measured are between different points on the same energy surfaces rather than an interchange between surfaces. The effect of a strain is to warp the surfaces, lowering one part with respect to another. This causes a flow from the higher energy-momentum region to the lower energy regions. The holes

change momentum directions near the impurity atoms by being captured in one of the excited states. This can happen with only a small number of collisions with phonons since the energies of the holes and the excited states are not very different. To leave the orbit, however, requires thermal energy to overcome the binding energy of the state, and this energy represents the activation energy measured. As the doping increases the activation energy decreases, and for a doping of 3×10^{19} boron atoms per cc it disappears entirely.

The activation energies for the relaxation time τ_1 of the shearing mode are in good agreement with the infrared measurements for the largest orbits in boron and gallium. The energy levels of the ground state—innermost orbit—and the excited states in relation to the band edge have been discussed by Kohn.¹³ These energy differences were measured by infrared absorption. The values of 0.0012 and 0.0035 eV agree well with the largest orbits, lowest energies, for the measured excited states. At lower temperatures, the relaxation times for the primary modes for both boron and gallium become so large that other processes take over. For boron doping, the next process is another excited state having the constants of Eq. (20), while for gallium

¹³ H. J. Hrostowski and R. H. Kaiser, *Bull. Am. Phys. Soc.* [2] **2**, 66 (1957); see also W. Kohn in *Solid State Physics*, edited by F. Seitz and D. Turnbull (Academic Press, Inc., New York, 1957), Vol. 5, p. 257.

doping it appears to be a process without activation energy such as elastic scattering by the impurity atoms.

Another verification that the processes observed are the excited states comes from the high-temperature values of τ_1 and τ_1' for both boron and gallium doping. The frequency with which an orbit is traversed is given by

$$f = \delta E / \hbar \doteq 2.8 \times 10^{11} \text{ cycles/sec (boron)} \\ \doteq 8.4 \times 10^{11} \text{ cycles/sec (gallium)} \quad (26)$$

for the first— τ_1 —process. The time of a cycle is the inverse of these values and the measured constants of 1.3×10^{-12} sec (boron) and 5×10^{-13} sec (gallium) indicate that the transfer of momentum at high temperatures takes place between points that are about one-third of a complete orbit apart. Since the shearing stress raises or lowers the energy surfaces along $\langle 111 \rangle$ directions, the closest equivalent positions are 109° apart or about one-third of a complete cycle. The second process τ_1' of Eq. (20) indicates that the hole traverses two-thirds of a much larger orbit before it transfers its momentum.

As the doping increases, the impurity atoms come so close together that bound orbits are no longer possible. In this region the only process left is the elastic scattering by the ionized impurities which follows the law of Eq. (17). If we use the measured relaxation time of 10^{-13} sec for the impurity doping of 3×10^{19} boron atoms per cc, and calculate the velocity from the equation

$$\frac{1}{2} m^* V^2 = 0.6 W_F = \frac{3}{10} (\hbar^2 / m^*) (3\pi^2 N)^{2/3}, \quad (27)$$

one finds for the scattering radius R the value of 8.5×10^{-8} cm. Comparing the relaxation time 10^{-13} with the total relaxation time from the conductivity Eq. (16) it appears that about 1 out of 10 collisions results in a change of position on the surface.

The theoretical situation for the change in moduli due to doping for *p*-type silicon is far from satisfactory. Three theoretical derivations^{1,14,15} have been given for the change in shearing modulus. The first solution¹ assumes spherical energy surfaces, as shown by the dashed lines of Fig. 6, and limits consideration to the heavy hole surface. The second solution¹⁴ takes account of the curvature of the two surfaces. In the degenerate range these solutions reduce to the forms

$$\Delta c_{440} = - \frac{(8\pi/3)^{2/3} m^* d^2 N^{1/3}}{5\hbar^2} \\ = \frac{-0.825 m^* d^2 N^{1/3}}{\hbar^2} \text{ (Keyes),} \quad (28)$$

$$\Delta c_{440} = (-2.38 m^* N^{1/3} d^2 / \hbar^2) \text{ (Bir and Tursunov).} \quad (29)$$

TABLE I. Values of Δc_{44} at 1.5°K for various dopings.

Doping $\Delta c_{44} \times 10^{-9}$	Boron doping				Gallium doping
	3×10^{19}	10^{19}	2.5×10^{18}	5×10^{17}	1.5×10^{18}
	17.9	12.4	13.5	10.5	17.2

Table I shows measurements for Δc_{44} at 1.5°K for different dopings for boron and one value for gallium doping.

In the degenerate region from 10^{19} to 3×10^{19} boron atoms per cc, the variation is proportional to the one-third power of the doping level in agreement with Eqs. (29) and (30). Taking m^* as $0.44m_0$ as an average value for the two surfaces, the deformation potential values are

$$d = 17.2 \text{ eV (Keyes);} \quad (30)$$

$$d = 10.1 \text{ eV (Bir and Tursunov).}$$

A third calculation has recently been made¹⁵ which yields values close to the value given by Keyes. Csavinszky and Einspruch¹⁵ have considered the spin-orbit coupled band in addition to the two degenerate bands but have assumed spherical symmetry of the bands. For doping up to 10^{19} boron atoms per cc, the two upper bands are sufficient for the calculation and the result obtained is

$$\Delta c_{440} = - \frac{1}{5} \left(\frac{8\pi}{3} \right)^{2/3} \frac{d^2}{\hbar^2} [m_{v_1} N_1^{1/3} + m_{v_2} N_2^{1/3}], \quad (33)$$

where $m_{v_1} = 0.49m_0$ is the heavy hole mass and $m_{v_2} = 0.16m_0$ is the light hole mass. Since

$$N_1 / N_2 = (m_{v_1} / m_{v_2})^{3/2} = 5.35, \quad (34)$$

$N_1 = 0.85N_0$ and $N_2 = 0.15N_0$. Hence, for a doping of 10^{19} boron atoms per cc, the value of $d = 15.4$ eV.

However, the larger values measured at the lower dopings at 1.5°K—for which asymptotic values have not been reached—and the large variation with temperature shown by Fig. 8(b) cast doubt on the validity of these calculations. It is conjectured that there is a temperature variation of the position of the holes on the energy surfaces and at low temperatures it seems likely that the heavy holes collect near the $\langle 111 \rangle$ positions while light holes collect near the $\langle 100 \rangle$ positions. As seen from Fig. 6, lower part, which shows the cross sections of the energy surfaces a constant distance below the origin, the heavy-hole $\langle 111 \rangle$ positions and the light-hole $\langle 100 \rangle$ positions are farthest from the origin and require electrons of higher momentum to reach the surface. Hence, if momentum is equalized in all directions, the surfaces near the origin should be filled up to a level higher than those far away and hence the $\langle 111 \rangle$ positions for the heavy-hole surface and the $\langle 100 \rangle$ positions for the light-hole surface should have the lower energies. At very

¹⁴ G. L. Bir and A. Tursunov, Fiz. Tverd. Tela 4, 2625 (1962) [English transl.: Soviet Phys.—Solid State 4, 1925 (1963)].

¹⁵ P. Csavinszky and N. G. Einspruch, Phys. Rev. 132, 2434 (1963).

low temperatures, holes tend to congregate in these directions.

If this conjecture is correct, the change in modulus for the heavy-hole surface should follow that for germanium, as given by Eq. (12), while that for the light-hole surface should follow Eq. (8) with kT replaced by (10), for the low temperatures, giving

$$\Delta c_{110} = -\frac{16}{3} \left(\frac{\pi}{3}\right)^{2/3} \frac{m^* N^{1/3} \Phi^2}{h^2}. \quad (31)$$

If we take an average value of 15 eV for the shear deformation potential d , the indicated change in modulus from Eq. (12)—using $m^* = 0.49m_0$ and $N = 0.85N_0$, i.e., 2.12×10^{18} heavy holes—is 26.5×10^9 dyn/cm², which is not out of line with the values of Fig. 8(b) extrapolated to lower temperatures. For higher doping levels this effect disappears since the momentum differences for the various positions become smaller.

Another piece of evidence that the light holes congregate along $\langle 100 \rangle$ positions at low temperatures is furnished by the nearly constant relaxation time of

Fig. 11 for longitudinal waves propagated along the $\langle 100 \rangle$ direction. The data of Fig. 12 show that p -silicon with boron becomes degenerate for a doping of 3×10^{19} atoms per cc. This is taken to mean that the impurities are near enough together to prevent any excited state orbits around the boron atoms. The smallest orbits will be executed by the heavy holes and hence they will reach degeneracy at a higher doping level than the light hole surface. With a mass ratio of 0.49 to 0.16 or 3.06, the radius will be this factor larger for the light-hole surface. Hence, this surface should become degenerate for a doping of

$$3 \times 10^{19} / (3.06)^3 \doteq 10^{18} \text{ boron atoms per cc.} \quad (32)$$

Therefore, the constant relaxation time of 4.2×10^{-12} sec for a sample doped with 2.5×10^{18} boron atoms per cc is a confirmation that, at low temperatures, a longitudinal stress along the $\langle 100 \rangle$ axis actuates mostly light holes.

If the relaxation time is due to scattering of light holes by impurities, calculations indicate that the scattering radius is about 5×10^{-8} cm, in good agreement with the value obtained for the degenerate heavy-hole surface.

Distribution Functions for the Number of Distinct Sites Visited in a Random Walk on Cubic Lattices: Relation to Defect Annealing*

J. R. BEELER, JR.

Nuclear Materials and Propulsion Operation, General Electric Company, Cincinnati, Ohio

(Received 17 January 1964)

Distribution functions for the number of distinct sites $S(n)$ visited by a point defect executing a symmetric random walk of n jumps on two- and three-dimensional lattices were computed using the Monte Carlo method. The square planar, simple cubic, bcc, and fcc lattices were treated. In three dimensions, the normal distribution appears to describe $S(n)$ for $n > 10^4$ jumps and at 10^4 jumps the derivative $d\bar{S}(n)/dn$ of the average number, $\bar{S}(n)$, of distinct sites is within 0.5% of the value given by Vineyard's exact asymptotic solution. The defect annealing rate was computed using the $S(n)$ distribution in a simple example and this result compared with an analog Monte Carlo solution. The comparison indicated that fluctuations in the initial defect concentration must be considered in computing the initial annealing rate and the mobile defect concentration as a function of time. After 500 jumps the annealing rate, but not the concentration, can be closely approximated without accounting for fluctuations in the initial concentration.

1. INTRODUCTION

IN a monatomic crystal, the migration of a defect, such as a vacancy or an interstitial atom, proceeds as a symmetric random walk¹ on the crystal lattice. The rate at which mobile defects are annihilated or trapped at point sinks is proportional to the rate at which they

encounter fresh sites which have not been visited previously. Damask and Dienes² will treat the physical side of this process in a forthcoming book. On the basis of a Monte Carlo study, Beeler and Delaney³ concluded that the average number of distinct sites, $\bar{S}(n)$, visited by a point defect in either a symmetric or an asymmetric random walk of n jumps was of the form,

$$\bar{S}(n) = An^k \quad (1)$$

* Work supported by the U. S. Atomic Energy Commission.

¹ In this discussion a symmetric random walk is one wherein the jump probabilities for each possible jump direction are equal and constant. The vacancy random walk in an alloy is in general asymmetric because of its ordering energy, i.e., the jump probabilities for each possible direction are not equal and also depend upon the position of the vacancy.

² A. C. Damask and G. J. Dienes, "Point Defects in Metals" (to be published).

³ J. R. Beeler, Jr., and J. A. Delaney, Phys. Rev. **130**, 962 (1963); J. R. Beeler, Jr., U.S.A.F. Report ASD-TDR 63-215 (unpublished).